

I. Llamas-Garro^{1*}, Z. Brito-Brito^{1*}, F. Mira¹, Marcos T. de Melo^{2*}, Jung-Mu Kim³

¹ Centre Tecnològic de Telecomunicacions de Catalunya (CTTC/CERCA), Castelldefels, Barcelona, Spain

² Departamento de Eletrônica e Sistemas, Universidade Federal de Pernambuco, Recife, Brasil

³ Division of Electronic Engineering, Jeonbuk National University, Jeonju, Republic of Korea

* Senior Member, IEEE

Received, revised, accepted, published, current version. (Dates will be inserted by IEEE).

Abstract—A microwave planar resonator sensor design supporting spoof surface plasmon waves is used for wafer dielectric characterization. The proposed circuit guides the microwave as a surface wave across the metal signal line, from port to port of the device. The surface wave effectively interacts with the sample being measured, placed on top of the planar sensor. The proposed planar sensor is fabricated on an RF-35 substrate, resulting in a low-cost implementation. The sensor is used to discriminate between wafers with different dielectric permittivity and thickness. Quartz, borosilicate, BK7 glass and Silicon wafers have been characterized using the proposed sensor. The sensor resonant frequency and losses change according to the permittivity and the thickness of the samples, with an achieved sensor sensitivity of 60.22 MHz/ ϵ_r .

Simulation and measurements demonstrate that the proposed spoof surface plasmon resonator sensor can be used to create a high sensitivity sensor for dielectric material characterization. The dielectric constant and loss tangent of the samples are inferred from a polynomial fit obtained from sample simulations and confirmed through measurements.

Index Terms— Dielectric properties, material characterization, resonator sensor, spoof surface plasmon waves.

I. INTRODUCTION

Surface plasmon phenomena has been widely used for sensing at optical wavelengths, using the well-known Kretschmann [1] and Otto [2] configurations, that allow the excitation of surface plasmon oscillations, widely used for sensing applications. The surface plasmon evanescent wave propagates adjacent to a metal and dielectric interface, high sensitivity sensor chips supporting the surface plasmon effect can be fabricated using nanotechnology [3].

To achieve spoof surface plasmon propagation at microwave frequencies, a periodical corrugation of the metal signal line, including holes or grooves has been proposed [4]. The geometry dependency on the spoof surface plasmon excitation makes it possible to develop circuits and transmission lines at microwave frequencies [5]. Many works related to surface plasmon microwave transmission lines, filters and antennas have been reported [4-12].

Microwave resonator-based sensors produce a resonance shift with an associated quality factor, according to the sample under test dielectric constant and loss tangent, respectively. Resonator-based sensors have been used in material characterization with high accuracy and sensitivity [13]. Developed microwave resonator-based sensors include implementations using substrate integrated waveguide (SIW) [14], split ring resonator (SRR) [15], metamaterial resonator (MTM) [16], LC resonator [17] and fractal resonator [18,19]. An overview of resonator-based sensors can be found in [13].

Recently, the work reported in [5] shows a microwave surface plasmon transmission line using an open cross structure. In this paper, a resonator is formed inspired on the transmission line described in [5] and used to form a high sensitivity low-cost sensor. The proposed microwave spoof surface plasmon sensor for dielectric material

characterization is used to measure four-inch wafer samples with different permittivity and thickness. The dielectric constant and loss tangent of each wafer sample is calculated using a polynomial fit obtained from sample simulations. The purpose of this work is to allow discriminating between different wafers at the laboratory, i.e., if the wafer material is unknown, the wafer is placed over the proposed low-cost sensor and the sensor response will swiftly allow identifying the material the wafer is made from.

This work starts with the design and simulation of the surface plasmon microwave resonator-based sensor in section II, the fabrication and measurements are shown in section III, results and discussion are provided in section IV; conclusions of this work can be found in section V.

II. DESIGN AND SIMULATION

To design the proposed spoof surface plasmon resonator-based sensor, the open-cross unit cell reported in [5] is used. Simulations are performed using Keysight ADS and a substrate with dielectric constant $\epsilon_r=3.5$, loss tangent $\tan\delta=0.0018$ and dielectric thickness of 1.52mm, corresponding to the RF-35 microwave laminate. The spoof surface plasmon transmission line is made of copper, with a conductivity of 5.87×10^7 [S/m], and 35 μm thickness. The layout of the proposed sensor is shown in Fig. 1a, the size of the resonator shown in Figs. 1a and 6 is fixed to resonate at 4.3 GHz, Fig. 1b shows the current distribution at 4.3 GHz, where the maximum current density is found at the resonator used for sensing, located at the center of the circuit.

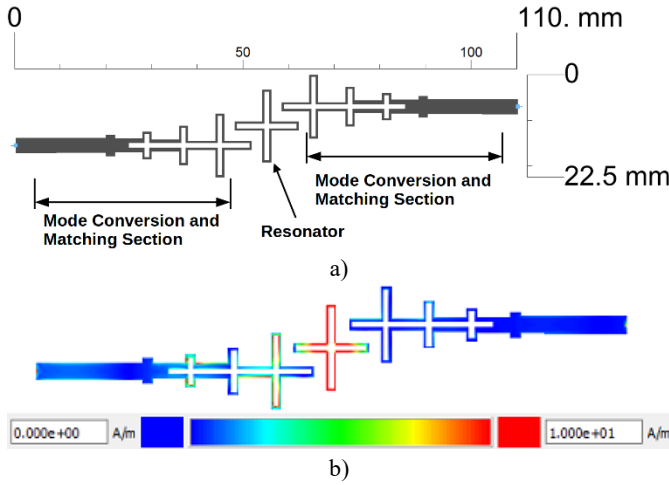


Fig. 1. Signal line of the spoof surface plasmon resonator-based sensor a) layout b) current distribution at 4.3 GHz.

The spoof unit cell (k_y) used to form the sensor is shown in Fig. 2, the dispersion curve of the spoof unit cell shown in Fig. 3 is obtained using the eigenmode solver of ANSYS HFSS. According to the dispersion curve in Fig. 3, the spoof unit cell dispersion characteristic deviates from the light line (k_0). Thus, the spoof unit cell in Fig. 2 propagates as a slow wave, leading to high electromagnetic field confinement [20-23]. Since $k_y > k_0$, there is a mismatch between wave vectors k_y and k_0 . Wave vector matching is achieved using a gradual transition from microstrip to the spoof surface plasmon transmission line, achieved by increasing the size of the unit cell gradually [20-23], corresponding to the mode conversion and matching section shown in Figs. 1a and 6.

The microwave spoof surface plasmon based resonator sensor concentrates the electromagnetic field near the open-cross structure as discussed in [4-12], and shown in Fig. 1b, considering the proposed resonator structure in this work.

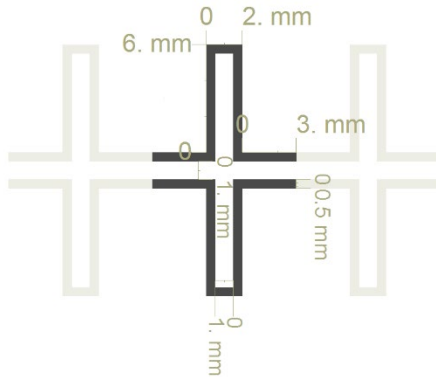


Fig. 2. Spoof unit cell.

When a dielectric sample is placed above the resonator, the sample produces a resonant frequency shift and quality factor change associated to the sample under test [24-30].

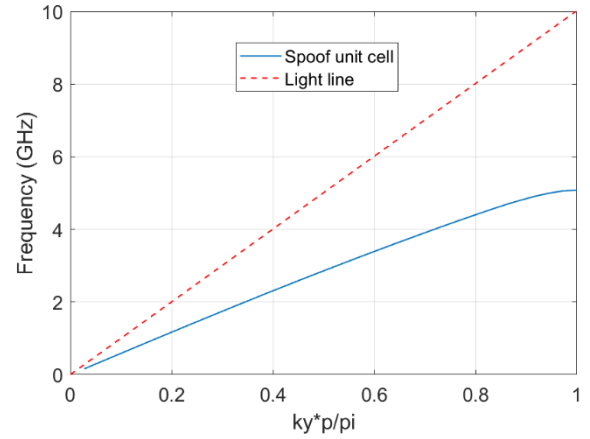


Fig. 3. Dispersion curve of the spoof unit cell.

The simulated S-parameters of the sensor with different samples under test are shown in Figs. 4 (S_{11}) and 5 (S_{21}). The resonant frequency and quality factor have specific values for each wafer under test, according to sample dielectric permittivity and thickness.

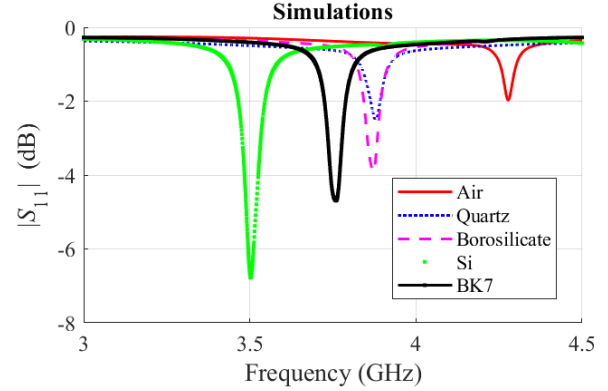


Fig. 4. S_{11} Simulated results.

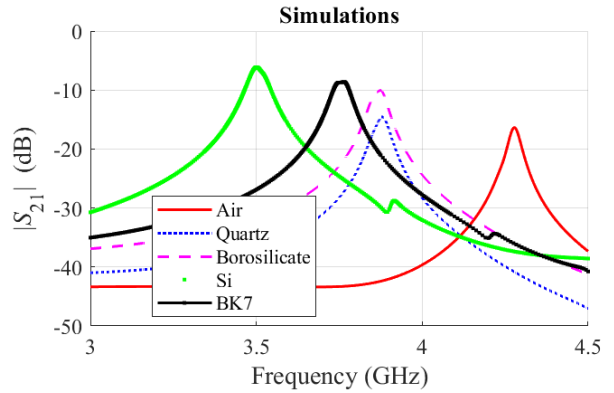


Fig. 5. S_{21} Simulated results.

III. FABRICATION AND MEASUREMENTS

The sensor has been manufactured using a CNC prototyping machine on an RF-35 substrate with SMA connectors. The substrate has a metal bottom layer, the central coaxial pin of the SMA connector is soldered to the signal line, the exterior coaxial casing is soldered to the bottom metal plate. Dimensions of the device are 110 x 62 mm. Experimental results consist of measurements using a PicoVNA vector network analyzer operating up to 6 GHz after a SOLT

calibration. Fig. 6 shows the manufactured sensor prototype, and Fig. 7 shows the measurement setup.

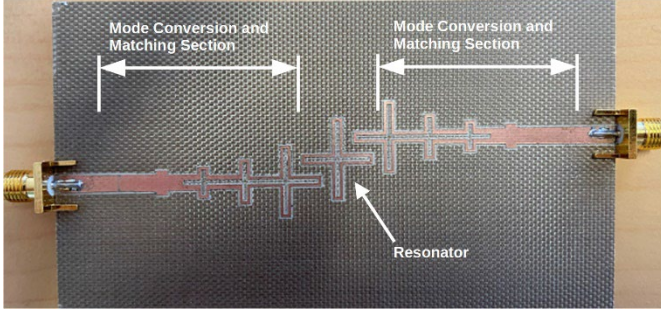


Fig. 6. Fabricated spoof surface plasmon resonator-based sensor.

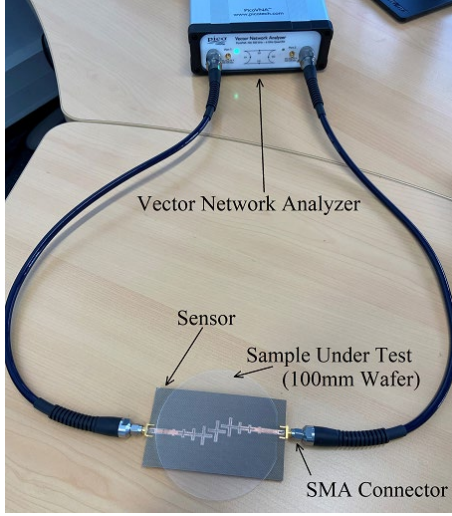


Fig. 7. Experimental setup to discriminate between four-inch wafers using the proposed spoof surface plasmon microwave sensor.

To validate the sensor, wafers with well-known dielectric permittivity properties are measured. As shown in Figs. 8 and 9, sample wafers under test, placed on top of the sensor produce frequency and quality factor or loss shift with respect to the sensor response without any sample under test. The comparison between experimental and simulated resonance frequencies for the different samples are summarized in Table 1.

Table 1. Spoof surface plasmon sensor simulated and measured resonant frequencies.

Sample	Simulated (GHz)	Measured (GHz)
No sample (air)	4.27	4.29
Quartz	3.88	3.90
Borosilicate	3.87	3.83
BK7	3.76	3.53
Si	3.50	3.42

IV. RESULTS AND DISCUSSIONS

Resonant frequency and quality factor characteristics are measured according to each sample under test. The dielectric constant sample values are varied in simulations between 2 and 16 as shown in the

polynomial fit curves of Fig. 10, defining the dielectric constant versus resonant frequency characteristics of the proposed planar spoof surface plasmon sensor.

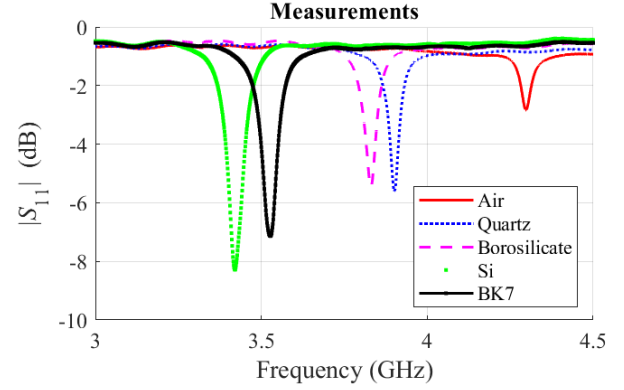


Fig. 8. S_{11} Measured results.

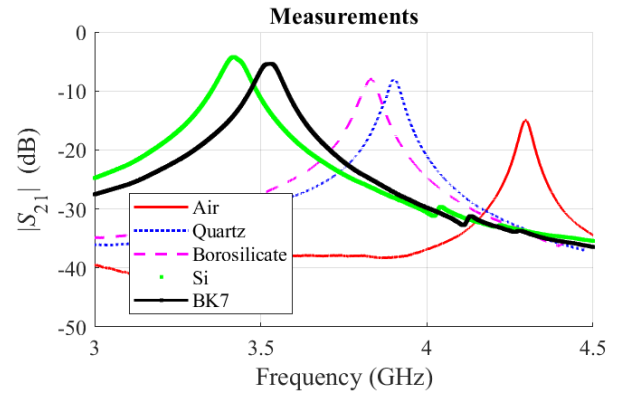


Fig. 9. S_{21} Measured results.

All wafer samples measured have a diameter of 100 mm. The dielectric constant of the 500 μm thick sample can be calculated or predicted according to eq (1), where f_r is the resonant frequency of the sensor with the sample under test.

$$\epsilon_r = -28.997f_r^3 + 353.286f_r^2 - 1444.31f_r + 1983.592 \quad (1)$$

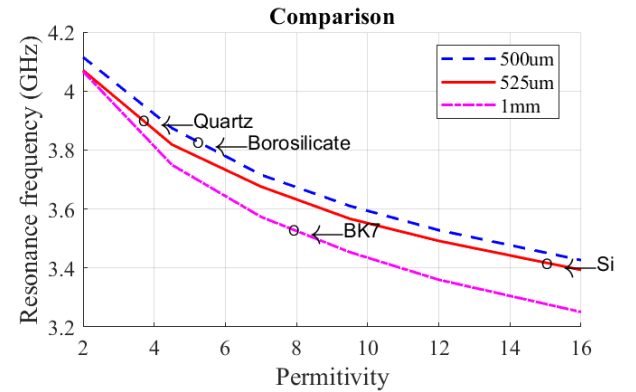


Fig. 10. Measured (dots) and simulated (lines) dielectric constant vs resonance frequency comparison.

The dielectric constant of the 525 μm thick sample can be calculated or predicted according to eq (2).

$$\varepsilon_r = -29.877f_r^3 + 361.955f_r^2 - 1470.516f_r + 2005.527 \quad (2)$$

The dielectric constant of the 1000 μm thick sample can be calculated or predicted according to eq (3).

$$\varepsilon_r = -20.211f_r^3 + 241.999f_r^2 - 972.932.668f_r + 1315.71(3)$$

Table 2 contains the comparison between dielectric constant reference range found in literature and the measured dielectric constant values for each sample under test. The main objective of this work is to discriminate between wafer materials at the laboratory with the proposed non-invasive sensor.

Table 2. Comparison between reference values and measured dielectric constant.

Sample	Thickness (μm)	Reference values	Measured
Quartz	525	3.7-3.9 [30-33]	3.56
Borosilicate	500	4-8[34-36]	5.08
BK7	1000	4-8[34-36]	7.77
Si	525	11.4-11.8[37-39]	14.89

To estimate the loss tangent of the sample it is necessary to calculate the unloaded quality factor of the resonator [40-42].

The loaded quality factor can be calculated directly from the measurement of S_{21} [40,41], using eq (4), the loaded quality factor includes the external coupling to the resonator.

$$Q_l = \frac{f_0}{BW_{3dB}} \quad (4)$$

where f_0 is the resonant frequency of the weakly coupled resonator, BW_{3dB} is the bandwidth taken at 3dB from the minimum insertion loss at the resonant frequency.

The unloaded quality factor, which relates only to the energy stored in the resonator, is a direct measure of the losses in the resonator-based sensor circuit, and can be calculated using the loaded quality factor [40,41], according to eq (5)

$$Q_0 = \frac{Q_l}{1 - |S_{21}|} \quad (5)$$

where $|S_{21}|$ is the absolute magnitude of S_{21} at the resonant frequency. The loss tangent ($\tan\delta$) can be calculated using the unloaded quality factor [40,41], by using eq (6)

$$\tan\delta = \frac{1}{Q_0} \quad (6)$$

The loaded and unloaded quality factors extracted from measurements are summarized in Table 3 for each sample under test. Table 3. Quality factor from measured S-parameters.

Sample	Q_l	Q_0
Quartz	86.6410	144.1344
Borosilicate	69.1042	114.9835
BK7	43.6714	94.3897
Si	41.6901	108.0118

Table 4 shows a comparison between the loss tangent reference range, found in literature and the measured loss tangent values for each sample under test.

Table 4. Comparison between reference values and measured loss tangent.

Sample	Reference values	Measured
Quartz	0.003-0.01 [31-34]	0.0069
Borosilicate	0.002-0.0143 [35-37]	0.0087
BK7	0.002-0.0143 [35-37]	0.0106
Si	0.002-0.05 [38,39,43]	0.0093

Sensor sensitivity can be calculated in four different ways [38], eq (7) relates the resonance frequency shift with the dielectric constant [38]

$$S = \frac{f_{air} - f_{sample}}{\varepsilon_{r_{sample}} - 1} \quad (7)$$

where $\varepsilon_{r_{sample}}$ is the dielectric constant of the sample, f_{air} is the resonant frequency of the sensor with no sample under test, and f_{sample} is the resonant frequency of the sensor with the sample under test. The sensitivity can be normalized to the resonance frequency of the sensor [38], by using eq (8)

$$S(\%) = \frac{f_{air} - f_{sample}}{f_{air}(\varepsilon_{r_{sample}} - 1)} \times 100 \quad (8)$$

Another formula to calculate sensor sensitivity, relates the resonance frequency shift to the dielectric constant change [38], as described in eq (9)

$$S = \frac{f_{air} - f_{sample}}{\Delta\varepsilon_{r_{sample}}} \quad (9)$$

where $\Delta\varepsilon_{r_{sample}}$ is the dielectric constant range of the sample under test. Finally, it is possible to calculate sensor sensitivity by using the slope of the line that fits the curve of the dielectric constant versus resonant frequency characteristic [18], as described in eq (10)

$$S = \text{slope of the linear fitting curve} \quad (10)$$

Table 5 provides a comparison of the proposed sensor for large sample sizes with other designs available in the literature, sensor sensitivity comparison is done using eq (7) to eq (10). The proposed sensor supporting spoof surface plasmon propagation achieves high sensitivity when compared to other implementations, since the microwave signal effectively propagates along the signal line, resulting in a high electromagnetic field interaction with the sample.

V. CONCLUSIONS

A low-cost, non-invasive, high sensitivity microwave planar sensor design, consisting of an open-cross resonator formed on a transmission line supporting spoof surface plasmon waves is used to characterize dielectric materials with dielectric constants ranging from 2 to 16. The results demonstrate that the proposed spoof surface plasmon sensor achieves high sensitivity when compared with other planar sensors available in the literature. The high sensitivity is achieved since the microwave signal used for sensing, propagates as a spoof surface plasmon wave across the sensor transmission line, thus the electromagnetic field effectively interacts with the sample under test. The proposed sensor is used to discriminate effectively between wafer materials at the laboratory.

Table 5. Sensor sensitivity comparison.

Reference	Technology	Sensitivity (MHz/ ϵ_r)			
		eq (7)	eq (8)	eq (9)	eq (10)
[14]	SIW	27.31	0.16	27.77	25.7
[15]	SRR	19.48	0.25	27.77	19.74
[16]	MTM	7	0.27	7	7
[17]	LC	8.14	0.43	12.9	8.12
[18]	Fractal	6.8	1.21	7.8	7
This paper	SSP	60.22	1.4	64.52	48.35

ACKNOWLEDGMENT

This work was funded by the IN CERCA grant from the Secretaria d'Universitats i Recerca del departament d'Empresa i Coneixement de la Generalitat de Catalunya. This work was supported in part by project PID2020-113832RB-C22 funded by MCIN/AEI/10.13039/501100011033 and the National Research Foundation of Korea (NRF), grant funded by the Korean government (MSIT) (No. 2021R1A4A1032234).

REFERENCES

- [1] E. Kretschmann, "Determination of optical constants of metals through the stimulation for surface plasma oscillations," *Z. Phys.* 241, 313–324 (1971).
- [2] A. Otto, "Excitation of nonradiative surface plasma waves in silver by the method of frustrated total reflection," *Z. Phys.* 216, 398–410 (1968).
- [3] E. Fontana, J. Mu-Kim, I. Llamas-Garro, G. Oliveira Cavalcanti, Microfabricated Otto chip device for surface plasmon resonance based optical sensing, *Applied Optics*, Vol. 54, No. 31, pp. 9200–9204, November 2015.
- [4] Liu, X., Zhu, L., Wu, Q. & Feng, Y. Highly confined and low-loss spoof surface plasmon polaritons structure with periodic loading of trapezoidal grooves. *AIP Advances* 5, 077123 (2015).
- [5] Zhang, Xue-Feng, Jian-Xin Chen, Rui-Feng Gao, Chen Xu, and Zhi-Hua Bao. "Differential Surface Plasmon Polaritons Transmission Line with Controllable Common Mode Rejection." *Scientific Reports* 7, no. 1 (June 7, 2017): 2974. <https://doi.org/10.1038/s41598-017-03242-6>.
- [6] Yin, J. Y., Ren, J., Zhang, H. C., Pan, B. C. & Cui, T. J. Broadband frequency-selective spoof surface plasmon polaritons on ultrathin metallic structure. *Sci. Rep.* 5, 8165 (2015).
- [7] Pantoja, M. F., Jiang, Z. H., Werner, P. L. & Werner, D. H. On the use of subwavelength radial grooves to support spoof surface plasmon-polariton waves. *IEEE Microw. Wireless Compon. Lett.* 26, 861–863 (2016).
- [8] Zhao, L. et al. A novel broadband band-pass filter based on spoof surface plasmon polaritons. *Sci. Rep.* 6, 36096 (2016).
- [9] Qiu, T., Wang, J., Li, Y. & Qu, S. Circulator based on spoof surface plasmon polaritons. *IEEE Antennas Wireless Propag. Lett.* 99, 1–4, doi:10.1109/LAWP.2016.2605738 (2016).
- [10] Liang, Y., Yu, H., Zhang, H. C., Yang, C. & Cui, T. J. On-chip sub-terahertz surface plasmon polariton transmission lines in CMOS. *Sci. Rep.* 5, 14853 (2015).
- [11] Ma, H. F., Shen, X., Cheng, Q., Jiang, W. X. & Cui, T. J. Broadband and high-efficiency conversion from guided waves to spoof surface plasmon polaritons. *Laser Photonics Rev.* 8, 146–151 (2014).
- [12] Tang, W. X., Zhang, H. C., Ma, H. F., Jiang, W. X., and, Cui, T. J. "Concept, theory, design, and applications of spoof surface plasmon polaritons at microwave frequencies". *Advanced Optical Materials*, 2019, vol. 7, no 1, p. 1800421.
- [13] Alahnomi, Rammah Ali, Zahriladha Zakaria, Zulkalnain Mohd Yusoff, Ayman Abdulhadi Althwayb, Ammar Alhegazi, Hussein Alsariera, and Norhanani Abd Rahman. "Review of Recent Microwave Planar Resonator-Based Sensors: Techniques of Complex Permittivity Extraction, Applications, Open Challenges and Future Research Directions." *Sensors* 21, no. 7 (January 2021): 2267. <https://doi.org/10.3390/s21072267>.
- [14] Memon, Muhammad Usman, and Sungjoon Lim. "Microwave Chemical Sensor Using Substrate-Integrated-Waveguide Cavity." *Sensors* 16, no. 11 (November 2016): 1829. <https://doi.org/10.3390/s16111829>.
- [15] Kiani, Sina, Pejman Rezaci, and Moein Navai. "Dual-Sensing and Dual-Frequency Microwave SRR Sensor for Liquid Samples Permittivity Detection." *Measurement* 160 (August 1, 2020): 107805. <https://doi.org/10.1016/j.measurement.2020.107805>.
- [16] Abdolrazzaghi, Mohammad, Mojgan Daneshmand, and Ashwin K. Iyer. "Strongly Enhanced Sensitivity in Planar Microwave Sensors Based on Metamaterial Coupling." *IEEE Transactions on Microwave Theory and Techniques* 66, no. 4 (April 2018): 1843–55. <https://doi.org/10.1109/TMTT.2018.2791942>.
- [17] Ebrahimi, Amir, James Scott, and Kamran Ghorbani. "Ultrahigh-Sensitivity Microwave Sensor for Microfluidic Complex Permittivity Measurement." *IEEE Transactions on Microwave Theory and Techniques* 67, no. 10 (October 2019): 4269–77. <https://doi.org/10.1109/TMTT.2019.2932737>.
- [18] C.P. do N. Silva, J.A.I. Araujo, M.S. Coutinho, M.R.T. de Oliveira, I. Llamas-Garro, and M.T. de Melo. "Multi-Band Microwave Sensor Based on Hilbert's Fractal for Dielectric Solid Material Characterization." *Journal of Electromagnetic Waves and Applications*, December 1, 2020. <https://doi.org/10.1080/09205071.2020.1861992>.
- [19] P. H. B. Cavalcanti Filho, J. A. I. Araujo, M. R. T. Oliveira, M. T. de Melo, M. S. Coutinho, L. M. da Silva, I. Llamas-Garro, Planar Sensor for Material Characterization Based on the Sierpinski Fractal Curve, *Journal of Sensors*, Vol. 2020, Article ID 8830596, December 2020.
- [20] Jaiswal, Rahul Kumar, Nidhi Pandit, and Nagendra Prasad Pathak. "Amplification of Propagating Spoof Surface Plasmon Polaritons in Ring Resonator-Based Filtering Structure." *IEEE Transactions on Plasma Science* 48, no. 9 (September 2020): 3253–60. <https://doi.org/10.1109/TPS.2020.3014856>.
- [21] Jaiswal, Rahul Kumar, Nidhi Pandit, and Nagendra Prasad Pathak. "Design and Performance Comparison of THz Slow Wave Spoof Plasmonic Metamaterial Based Transmission Lines." In 2019 IEEE Indian Conference on Antennas and Propagation (InCAP), 1–4, 2019. <https://doi.org/10.1109/InCAP47789.2019.9134556>.
- [22] Kumar Jaiswal, Rahul, Nidhi Pandit, and Nagendra Prasad Pathak. "Slow Wave Spoof Plasmonic Metamaterial Based Multi-Band Band-Stop Filter Using Complementary Split Ring Resonators." In 2019 IEEE MTT-S International Microwave and RF Conference (IMARC), 1–4, 2019. <https://doi.org/10.1109/IMARC45935.2019.9118762>.
- [23] Jaiswal, Rahul Kumar, and Nagendra P. Pathak. "Spoof Surface Plasmon Polaritons (SSPP) Based Multi-Band Bandpass Filter." In 2016 Asia-Pacific Microwave Conference (APMC), 1–4, 2016. <https://doi.org/10.1109/APMC.2016.7931393>.
- [24] Shete, Manisha, Makkattary Shaji, and Mohammad Jaleel Akhtar. "Design of a Coplanar Sensor for RF Characterization of Thin Dielectric Samples." *IEEE Sensors Journal* 13, no. 12 (December 2013): 4706–15. <https://doi.org/10.1109/JSEN.2013.2272120>.
- [25] U. C. Hasar and C. R. Westgate, "A broadband and stable method for unique complex permittivity determination of low-loss materials," *IEEE Trans. Microw. Theory Tech.*, vol. 57, no. 2, pp. 471–477, Feb. 2009.
- [26] A. M. Nicolson, "Measurement of intrinsic properties of materials by time domain techniques," *IEEE Trans. Instrum.*, vol. 1–19, no. 4, pp. 377–382, Nov. 1970.
- [27] J. Baker-Jarvis, E. Vanzura, and W. Kissick, "Improved technique for determining complex permittivity with the transmission/reflection method," *IEEE Trans. Microw. Theory Tech.*, vol. 38, no. 8, pp. 1096–1103, Aug. 1990.

-
- [28] M. Nakhkash, Y. Huang, and M. T. C. Fang, "A new free space technique for measuring the complex permittivity and thickness of materials," in *Proc. IEEE Nat. Conf. Antennas Propag.*, Mar. 1999, pp. 23–26.
- [29] H. Zhou, G. Lu, Y. Li, S. Wang, and Y. Wang, "An improved method of determining permittivity and permeability by S parameters," in *Proc. PIERS*, Mar. 2009, pp. 754–759.
- [30] W. B. Weir, "Automatic measurement of complex dielectric constant and permeability at microwave frequencies," *Proc. IEEE*, vol. 62, no. 1, pp. 33–36, Jan. 1974.
- [31] Ghodgaonkar, D.K., V.V. Varadan, and V.K. Varadan. "A Free-Space Method for Measurement of Dielectric Constants and Loss Tangents at Microwave Frequencies." *IEEE Transactions on Instrumentation and Measurement* 38, no. 3 (June 1989): 789–93. <https://doi.org/10.1109/19.32194>.
- [32] Kawabata, Hirokazu, Yoshio Kobayashi, and Syougo Kaneko, "Analysis of Cylindrical Cavities to Measure Accurate Relative Permittivity and Permeability of Rod Samples." In *2010 Asia-Pacific Microwave Conference*, 1459–62, 2010.
- [33] Yao, Yongliang, Hongling Cui, Junhu Wang, En Li, and Bingjie Tao. "Broadband Measurement of Complex Permittivity by an Open Resonator at 20–40GHz." In *2014 IEEE International Conference on Communication Problem-Solving*, 273–76, 2014. <https://doi.org/10.1109/ICCPS.2014.7062271>.
- [34] Kang, Tae-Weon, Jeong-Hwan Kim, Dong-Joon Lee, and No-Weon Kang. "Free-Space Measurement of the Complex Permittivity of Liquid Materials at Millimeter-Wave Region." In *2016 Conference on Precision Electromagnetic Measurements (CPEM 2016)*, 1–2, 2016. <https://doi.org/10.1109/CPEM.2016.7540566>.
- [35] Wang, Zhongjian, Yichen Hu, Hongkai Lu, and Fang Yu. "Dielectric Properties and Crystalline Characteristics of Borosilicate Glasses." *Journal of Non-Crystalline Solids*, *Proceedings of the 2005 International Conference on Glass*, 354, no. 12 (February 15, 2008): 1128–32. <https://doi.org/10.1016/j.jnoncrysol.2007.01.099>.
- [36] huanhuan, Wan, Zhang weijun, and Liu zhuofeng. "Fabrication and Characterization of Nickel-Gold Plateable LTCC Substrates Based on Borosilicate Glass/Al₂O₃ System." In *2018 19th International Conference on Electronic Packaging Technology (ICEPT)*, 1649–52, 2018. <https://doi.org/10.1109/ICEPT.2018.8480794>.
- [37] Schott, Technical Glasses, Physical and Technical Properties. https://www.schott.com/d/epackaging/2fbc7180-e37c-4209-9eec-617ad9208e51/1.4/final_schott_technical_glasses_row.pdf, 2014 (accessed 10 September 2021).
- [38] Krupka, Jerzy, Jonathan Breeze, Neil McN. Alford, Anthony E. Centeno, Leif Jensen, and Thomas Claussen. "Measurements of Permittivity and Dielectric Loss Tangent of High Resistivity Float Zone Silicon at Microwave Frequencies." In *2006 International Conference on Microwaves, Radar Wireless Communications*, 1097–1100, 2006. <https://doi.org/10.1109/MIKON.2006.4345377>.
- [39] Afsar, M.N., H. Chi, and X. Li. "Millimeter Wave Complex Refractive Index, Complex Dielectric Permittivity and Loss Tangent of High Purity and Compensated Silicon." In *Conference on Precision Electromagnetic Measurements*, 238–39, 1990. <https://doi.org/10.1109/CPEM.1990.110005>.
- [40] G. Matthaei, L. Young and E.M.T. Jones, "Microwave filters, impedance matching networks and coupling structures", Artech house Inc, 1964.
- [41] Jia-Sheng Hong and M.J. Lancaster, "Microstrip filters for RF/Microwave applications", John Wiley and Sons Inc, 2001.
- [42] Chen, Hetuo, Xuewen Fu, Qi An, Bin Tang, Shuren Zhang, Hao Yang, Yin Long, Mark Harfouche, Huolei Wang, and Yingxiang Li. "Determining the Quality Factor of Dielectric Ceramic Mixtures with Dielectric Constants in the Microwave Frequency Range." *Scientific Reports* 7 (October 26, 2017). <https://doi.org/10.1038/s41598-017-14333-9>.
- [43] Yang, Ru-Yuan & Hung, Cheng-Yuan & Su, Yan-Kuin & Weng, Min-Hang & Wu, Hung-Wei. (2006). Loss characteristics of silicon substrate with different resistivities. *Microwave and Optical Technology Letters*. 48. 1773 - 1776. 10.1002/mop.21786. DOI 10.1002/mop.21786.